A mass-preserving Sliding Mode Observer for Li-ion cells electrochemical model

Stefano Marelli, Matteo Corno

Abstract— **An advanced Battery Management System (BMS) is required to operate lithium-ion (Li-ion) batteries efficiently and safely. Such a BMS should estimate the cells internal states (residual charge, temperature, ions concentrations) accurately and, at the same time, with a reduced computational cost. In this work, the concentrations in a Li-ion cell are estimated via a Sliding Mode Observer (SMO) applied to the electrochemical Single Particle Model (SPM); thanks to the selected model solution technique, this setup offers accurate estimations of both distributed and bulk quantities, with high computation efficiency. An observability issue is encountered in a simple SMO application to SPM, which is overcome by a new two-step algorithm for the design of the observer gain matrix. This algorithm aims at preserving the total lithium mass estimated by the SMO. The proposed approach is validated in simulation with currents as high as 10C.**

I. Introduction

Lithium ion (Li-ion) batteries represent nowadays the most adopted technology for both (hybrid) electric vehicles and consumer electronics. In fact, they offer outstanding energy and power densities compared to other chemistries. However, the materials employed to manufacture Li-ion cells suffer from chemical instability and are subject to possible over-heating and even explosion. To deal with their nature, Li-ion cells require advanced Battery Management System (BMS) for accurate measurements, estimations and monitoring of the battery pack.

STILL SAME AS CDC UKF

Because of inaccuracies in the estimation, the current BMS design approach is often conservative; the BMS does not exploit the full potential of the battery. The key factors in operating a Li-ion cell are essentially the need for accurate modeling, parameters identification and state estimation.

A Li-ion cell is mainly composed of a negative and positive electrode, and a separator [1]. The electrodes have a lattice structure, in which active material (i.e. lithium) is stored, and are immersed in an (usually liquid) electrolyte. The separator is an electrical insulator which allows only the Li-ions to flow through it. During discharge, lithium diffuses to the surface of active material particles of the negative electrode and it undergoes the electron-generating reaction. Then, Li-ions, dissolved in the electrolyte, cross the separator, while electrons are conducted by the solid lattice to the current collector. Finally, both Li-ions and electrons reach the positive electrode and are reabsorbed in the active material particles. This process is called *dual-intercalation*, and is described with more detail for example in [2].

This work was supported by MIUR SIR project RBSI14STHV.

The authors are with the Department of Electronics, Information and Bioengineering, Politecnico di Milano, via G. Ponzio 34/5, 20133, Milan, Italy.

Email: {stefano.marelli,matteo.corno}@polimi.it

Li-ion cells models can be of various complexity, as shown in [3], starting from equivalent circuits, to advanced Computational Fluid Dynamics (CFD) models, that are extremely accurate, but at the price of high computational cost. In the aforementioned work, it was also shown how standard battery operations could be improved if limitations were applied to reactions overpotentials instead of just on terminal voltage (as done in current practice). This improvement can only be achieved if a sufficiently accurate model is selected, with insight on the electrochemical reactions taking place inside the cell. In particular, internal lithium concentration gradients represent a crucial information if one wants to effectively avoid reaching locally critical depletion levels [4]. The first-principle Pseudo 2-Dimensional (P2D) model originally formulated in [5], and later adopted in works such as [6], [7] and [2], is widely recognized as a valuable trade-off between modeling detail and computational cost. The P2D model, relying on Partial Differential Algebraic Equations (PDAEs), poses some limitation in terms of computational demands and observer formulation. The literature offers several methods to find approximated and/or reduced-order solutions to the whole model or just to the solid-phase diffusion dynamics [8]. For example, the Single Particle Model (SPM) [9] assumes each electrode as composed by a single spherical particle, thus neglecting the electrolyte dynamics. This model does not encompass concentrations gradients in longitudinal direction; as a consequence, it is accurate for low currents only. Another approach is to simplify the diffusion dynamics in the spherical particles radial direction. For example, [10] forces an assumption of parabolic or polynomial concentrations distribution in active material particles. Integral expressions for the response of reaction molar flux for short times and long times were, instead, introduced by [5]. Furthermore, [7] proposed a solid phase diffusion impedance model, and applied Finite Elements Method (FEM) on electrolyte phase. The present work employs a Finite Difference Method (FDM) space-discretization technique for the PDAEs as it allows for easy order rescaling and maintains the physical meaning of all the variables and parameters.

CITATIONS general SMO [11], [12]

SMO to battery, equivalent circuit, only SoC, reduce chattering with a self-adjusted switching gain [13]

State estimation techniques reflect the complexity and accuracy of the models they employ. One of the most successful

and well investigated approach employs the SPM [14]. Other works employ the P2D model by proposing different types of order reduction: [4] estimates the instantaneous available current; [15] estimates the bulk SoC using an Extended Kalman Filter (EKF) on a linearized version of the P2D model; [16] extends the estimation to the Li-ion concentrations using a Kalman Filter based on orthogonal collocation. The nonlinear nature of the cell dynamics may be better suited for nonlinear filtering techniques: [17] investigates the use of Unscented Kalman Filter (UKF) for SoC estimation in an simple equivalent circuit model, while [18] applies it to a volume-averaged electrochemical model. The previous results prove that the UKF approach [19] is an interesting tool to account for the cell nonlinear dynamics. The present work further extends the application of the UKF to the complete (i.e. not simplified) electrochemical P2D model. This not only enables the accurate estimation of bulk quantities, such as SoC, but also exploits the capability of the P2D model to estimate local concentration values in any point of the cell. The UKF approach has mainly three advantages: 1) it does not require a closed-form representation of the dynamics; this makes it very useful to avoid analytically solving the algebraic constraints, 2) it can be easily modified to account for soft-constraints that, as illustrated, improve the model observability, and 3) it is amenable to parallel implementation.

This paper is structured as follows. In Section II, the P2D model is recalled and space-discretized. In Section **??**, the main problems arising from applying the classical UKF to the P2D model are first introduced, then solved by implementing the concept of soft-constrained UKF; also, the results of UKF parallel implementation are shown. The new approach is fully validated in simulation in Section IV. Finally, conclusions are drawn in Section V.

II. Single particle model

In the SPM, the dual-intercalation process is described by a set of PDAEs, only considering the diffusion dynamics that take place inside the spherical particles, along the *radial direction r*; diffusion across the battery film thickness is neglected. The diffusion dynamics in the two electrodes is ruled by *Fick's law*:

$$\frac{\partial c_{s,i}}{\partial t} = \frac{D_{s,i}}{r^2}\frac{\partial}{\partial r}\left(r^2\frac{\partial c_{s,i}}{\partial r}\right) \tag{1}$$

where c_s is the concentration of lithium in solid phase, and subscript $i = \{n, p\}$ indicates negative or positive electrode, respectively; D_s is the solid phase diffusion coefficient. The boundary conditions at the particle core and surface are, respectively:

$$\left.\frac{\partial c_{s,i}}{\partial r}\right|_{r=0} = 0$$
$$\left.D_{s,i}\frac{\partial c_{s,i}}{\partial r}\right|_{r=R_{s,i}} = \frac{-j_i^{Li}}{a_{s,i}F}$$

where a_s is the specific interfacial area and F is Faraday's constant. j^{Li} is the molar flux at particle surface, and is related to the input current I as follows:

$$\begin{aligned} j_n^{Li} &= \frac{I}{a_{s,n}FA\delta_n} \\ j_p^{Li} &= -\frac{I}{a_{s,p}FA\delta_p} \end{aligned} \tag{2}$$

where A is the electrode plate area and δ is the electrode thickness. The overpotential η can be computed from the inversion of *Butler-Volmer kinetics equation*, under the commonly accepted hypothesis of equal charge transfer coefficients in the two electrodes ($\alpha_n = \alpha_p = 0.5$):

$$\eta_i = \frac{2RT}{F}\sinh^{-1}\left(\frac{F}{2j_{0,i}}j_i^{Li}\right)$$

where R is the universal gas constant; T is the lumped cell temperature; j_0 is the exchange current density. Finally, the output voltage is given by:

$$V = (U_p + \eta_p) - (U_n + \eta_n) - \frac{R_f}{A}I \tag{3}$$

where R_f is the film resistance of the electrode plate and U is the thermodynamic equilibrium potential, a non-linear function of surface concentration c_{ss}. In the following, the subscript *ss* denotes the superficial element of concentration, *i.e.* $c_{ss,i} = c_{s,i}(r = R_{s,i})$, while the subscript *sc* denotes the core element of concentration, *i.e.* $c_{sc,i} = c_{s,i}(r = 0)$.

It is also useful to introduce the definition of stoichiometry, that is the normalized version of concentration over the maximum value $c_{s,i}^{max}$:

$$\theta_{s,i} = \frac{c_{s,i}}{c_{s,i}^{max}}$$

and the definition of State of Charge (conventionally computed on negative electrode):

$$\mathrm{SoC} = \frac{\left(\frac{3}{R_{s,n}^3}\int_0^{R_{s,n}} r^2\theta_{s,n}\ \mathrm{d}r\right) - \theta_{s,n}^{0\%}}{\theta_{s,n}^{100\%} - \theta_{s,n}^{0\%}}$$

where $\theta_{s,n}^{0,100\%}$ are the values of stoichiometry, respectively, at 0 and 100% SoC.

The SPM is discretized in space and solved via *Chebyshev orthogonal collocation method*. Here we summarize only the main steps behind this approach, while the reader may refer to [16] for a complete discussion on the method and its computational details. Essentially, the proposed method consists in the following steps:

1) A proper change of variables is introduced and the diffusion equations are written accordingly.
2) A system of linear ODEs is obtained and solved thanks to Chebyshev differentiation matrices, which allow to approximate PDEs solutions as polynomials at the $N_c + 1$ Chebyshev nodes (here $N_c = 20$ is set).
3) The non-linear output equation of the model is analogous to (3) (that is, a function of the linear system outputs and of the input current).

As part of the first step introduced above, a new state vector is defined in place of $c_{s,i}$, with a suitable change of variables:

$$\omega_i = r c_{s,i} \tag{4}$$

so that the diffusion equation (1) can be rewritten, after defining $\rho = r/R_{s,i}$, as:

$$\frac{\partial \omega_i}{\partial t} = \frac{D_{s,i}}{R_{s,i}^2} \frac{\partial^2 \omega_i}{\partial \rho^2}. \tag{5}$$

Secondly, gradients of ω_i along ρ are approximated thanks to Chebychev differentiation matrices C_1 and C_2, for first and second derivative, respectively:

$$\frac{\partial \omega_i}{\partial \rho} \approx C_1 \omega_i \tag{6}$$

$$\frac{\partial^2 \omega_i}{\partial \rho^2} \approx C_2 \omega_i. \tag{7}$$

In this way, the system is formulated in state-space form as:

$$\begin{cases} \dot{\omega}_i = A_{\omega,i}\omega_i + B_{\omega,i} j_i^{Li} \\ c_{s,i} = C_{\omega,i}\omega_{s,i} + D_{\omega,i} j_i^{Li} \end{cases} \tag{8}$$

where $A_{\omega,i}$,$B_{\omega,i}$,$C_{\omega,i}$,$D_{\omega,i}$ are the state-space matrices obtained from manipulation of C_1 and C_2. $c_{s,i}$ is considered as the output of the reformulated linear system. Eventually, a single state vector Ω is defined as the concatenation of ω_n and ω_p. Also, since $c_{s,i}$ is a linear function of the state ω_i and of the input I, equation (3) can be properly rewritten to obtain the final state-space representation of the cell model:

$$\begin{cases} \dot{\Omega} = A_\Omega \Omega + B_\Omega I \\ V = h(\Omega, I) \end{cases} \tag{9}$$

where A_Ω is obtained by concatenating matrices $A_{\omega,i}$ and B_Ω by concatenating matrices $B_{\omega,i}$ and scaling them according to equations (2). The obtained model has a linear state transition equation and a non-linear output function.

III. Sliding Mode Observer Design

The objective of this section is to estimate concentrations inside the spherical particles, which are unmeasurable quantities, based on the SPM and measured output voltage. A generic SMO approaches this problem by implementing a copy of the model and injecting a discontinuous correction term on the state transition equation. Indicating with $\hat{\Omega}$ and $\hat{V}$, respectively, the estimated state and output of the system, the following observer structure is obtained:

$$\begin{cases} \dot{\hat{\Omega}} = A_\Omega \hat{\Omega} + B_\Omega I + M v \\ \hat{V} = h(\hat{\Omega}, I) \end{cases}$$

where v is the discontinuous injection term, while M is the observer gain matrix, to be designed so as to drive to zero in finite time the *sliding variable* defined as:

$$\sigma = e_V = V - \hat{V}$$

which is the output voltage estimation error. The injection term is simply given by:

$$v = \text{sign}(e_V).$$

Note that, since it is difficult to give a physical interpretation to a correction term on state Σ, the actual implementation of the SMO proposed here acts directly on $c_{s,i}$; details are skipped for the sake of brevity. In the following exemplifications, correction terms are thus applied on $c_{s,i}$, which can be better understood by the reader.

The proposed SMO is based on the following two assumptions:

Assumption 1: Since U_n and U_p, appearing in output function $h(\cdot)$, are monotonically decreasing functions, respectively, of $\theta_{ss,n}$ and $\theta_{ss,p}$ (see [6] for some examples of such functions for different cell chemistries), it is reasonable to assume that a positive error on V is due to a negative error on cs,n and to a positive error on cs,p. In symbols, this assumption can be expressed as:

$$e_V > 0 \Rightarrow \begin{cases} \hat{c}_{s,n} < c_{s,n} \\ \hat{c}_{s,p} > c_{s,p} \end{cases}.$$

This assumption extends the one made by [20] to the case with two electrodes.

Assumption 2: The "true" cell (in this work: the simulated system) is at steady-state at the beginning of the test, *i.e.* a sufficient time in rest condition has passed, so that inner concentration gradients are null. Thus, SMO initialization should be uniform in terms of c_s along r.

A. SMO with uniform correction

One simple choice for matrix M is a scalar gain m multiplying a vector of "+1"s in all N_c+1 positions corresponding to $c_{s,n}$ and "-1"s in all N_c+1 positions corresponding to $c_{s,p}$:

$$M = m \begin{bmatrix} +1 \\ \vdots \\ +1 \\ -1 \\ \vdots \\ -1 \end{bmatrix}. \tag{10}$$

This implies that the correction of concentrations takes place uniformly along r for all elements of both negative and positive electrodes, with proper sign, as depicted in Figure 1. However, the SPM is characterized by a poor

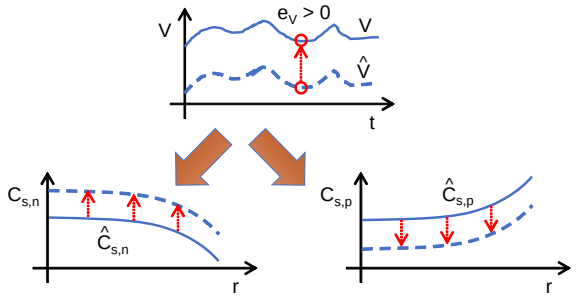

Fig. 1. Concentrations correction in SMO, with M designed as in (10).

observability of the core concentration of active material particles from the measured voltage, as analyzed by [14]. Also, the uniform injection mechanism in SMO does not guarantee the conservation of total lithium mass in the cell. In fact, concentration is corrected in the two electrodes with a certain gain, with proper sign, but without any information on how much lithium is withdrawn from an electrode and how much is supplied to the other one, due to the injection term (recall that, in general, the physio-chemical and geometrical characteristics of the two elecrode are different). Thus, without any additional enforcement of lithium mass conservation, the total mass of lithium in SMO soon moves from its initial value, and state estimate does not converge to an acceptable result. A simulation study is reported here to confirm this issue.

The test consists in a pulse discharge at 0-10C (i.e. 10 times the nominal current of the cell, defined as I/Q, where Q is the cell rated capacity), starting from a fully charged cell ($\text{SoC}_0 = 100\%$), with pulses and rests of 10s duration. The SMO is initialized with a 20% error in SoC ($\text{SoC}_{0,SMO} = 80\%$). The following state estimation errors are introduced, for surface and core concentrations, respectively, for both electrodes:

$$e_{ss,i} = c_{ss,i} - \hat{c}_{ss,i}$$
$$e_{sc,i} = c_{sc,i} - \hat{c}_{sc,i}$$

Although the sliding variable e_V is driven to zero in about 9s, as shown in Figure 2, the state estimates do not converge to the "true" values, as clear from Figures 3 and 4. This

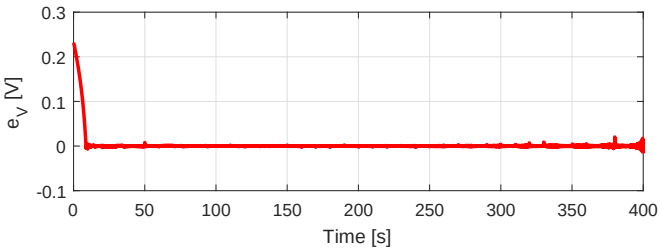

Fig. 2. Output voltage estimation error for SMO with uniform correction.

behavior is explained by investigating the number of moles of lithium stored in each electrode; for the SPM, this can be computed as:

$$n_{s,i} = \frac{3A\delta_i\varepsilon_{s,i}}{R_{s,i}^3}\int_0^{R_{s,i}} r^2 c_{s,i}\,\mathrm{d}r$$

where ε_s is the solid-phase volume fraction, while the total number of moles of lithium stored in the cell is the sum of those of the two electrodes:

$$n_s = n_{s,n} + n_{s,p}.$$

In order for n_s to remain constant, any variation in $n_{s,n}$ should be compensated by an equal and opposite variation in $n_{s,p}$, and *vice-versa*. Figure 5 shows the number of moles of lithium available in the two electrodes and in the cell during the previous test, for both simulated cell and SMO.

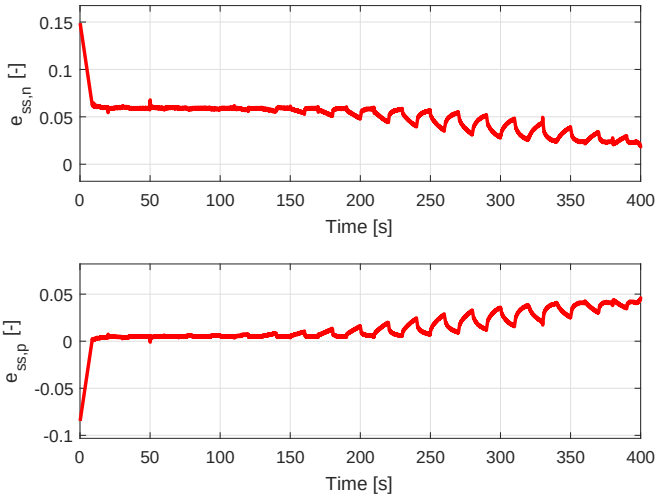

Fig. 3. Negative electrode state estimation errors for SMO with uniform correction (top: particle surface; bottom: positive electrode.

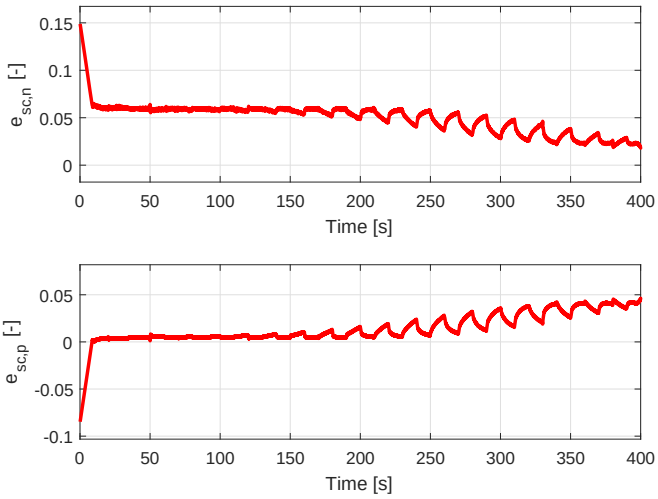

Fig. 4. Positive electrode state estimation errors for SMO with uniform correction (top: negative electrode; bottom: positive electrode).

In discharge conditions, as those considered here, negative electrode is emptying with lithium, while positive electrode is getting filled; however, here, there is a clear decrease in total number of moles of lithium in the first part of the simulation for SMO with uniform correction. This means that the variations in $n_{s,n}$ and $n_{s,p}$ are not balanced with such observer design.

B. SMO with mass-preserving correction

The algorithm proposed here has the objective of overcoming the above limitations of SMO applied to the SPM. It enforces total lithium mass conservation, by designing M according to the following two steps:

1) correct all $N_c + 1$ elements of $c_{s,n}$ as in (10);
2) correct each element k (for $k = 1..N_c + 1$) of $c_{s,p}$ enforcing null mass variation w.r.t. the k-th element of $c_{s,n}$.

Importantly, the correction on $c_{s,p}$ has the same sign as in (10), but with a pondered gain design. While step 1 above

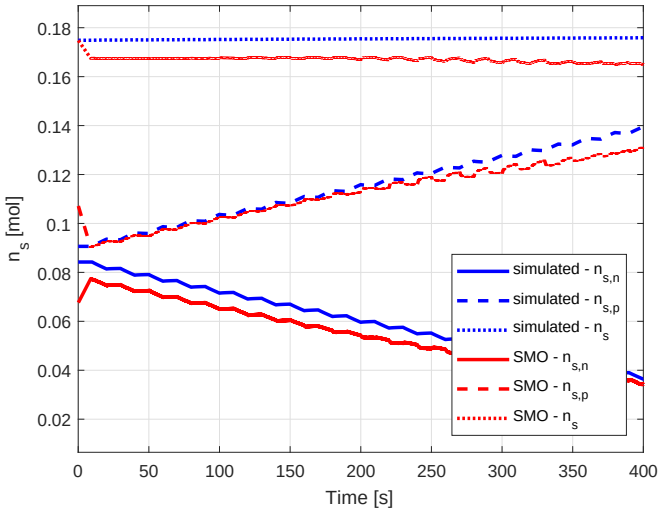

Fig. 5. Mass conservation problem in SMO with uniform correction: number of moles of lithium available in negative electrode, positive electrode and cell.

is trivial, step 2 needs an analysis on electrode properties. Although the SPM describes the dynamics of only one sphere in each electrode, the lattice structure is composed of thousands of millions particles. Based on the cell parameters, the number of active material spheres in each electrode can be computed as the ratio of effective electrode volume over the volume of an individual sphere:

$$N_i^{sph} = \frac{A\delta_i\varepsilon_{s,i}}{\frac{4}{3}\pi R_{s,i}^3}.$$

When the correction term is applied to the k-th element of $c_{s,n}$, a variation in lithium concentration is obtained (w.r.t. just the open-loop state transition), which is called $\Delta c_{n,k}$. This means that all spheres in negative electrode are receiving such a variation in concentration at position k along r (recall: SPM does not distinguish among spheres along x direction). The overall variation of the number of moles of lithium available in the negative electrode at position k is thus given by:

$$\Delta n_{n,k} = \Delta c_{n,k} N_n^{sph} V_{n,k}^{sec} \tag{11}$$

where $V_{n,k}^{sec}$ is the volume of the k-th spherical sector in negative electrode. To ensure mass conservation, the correction term of the k-th element of $c_{s,p}$ should lead to a variation in lithium moles equal and opposite to that of the k-th element of $c_{s,n}$:

$$\Delta n_{p,k} = -\Delta n_{n,k}.$$

Finally, with a similar reasoning as that applied to write (11), the corresponding variation in lithium concentration in positive electrode is found as:

$$\Delta c_{p,k} = \frac{\Delta n_{p,k}}{N_p^{sph} V_{p,k}^{sec}} = -\frac{\Delta c_{n,k} N_n^{sph} V_{n,k}^{sec}}{N_p^{sph} V_{p,k}^{sec}} \tag{12}$$

which is the correction term to be applied to the k-th element of $c_{s,p}$ to exactly balance the k-th injection term of of $c_{s,n}$. In this way, the total mass of lithium available in the cell is conserved. Notice that, as opposed to the strategy presented in Section III-A, the correction of concentrations is not uniform in positive electrode, and it is an explicit function of that applied to the negative electrode, as depicted in Figure 6. The following section validates this algorithm

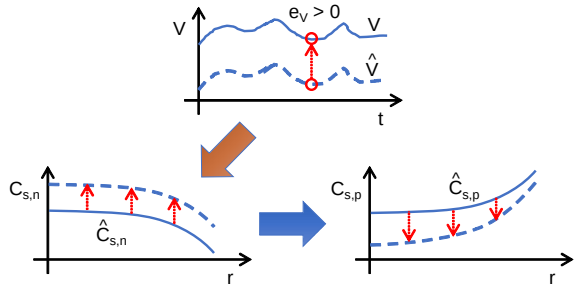

Fig. 6. Concentrations correction in SMO, with M designed as described in Section III-B.

with a simulation study.

IV. Validation

This section validates the mass-preserving SMO presented in the previous section. The considered test is the same as described in the previous section. Figure 7 shows the sliding variable in mass-preserving SMO, for different values of the scalar gain m (applied only on negative electrode, as explained earlier). The following considerations can be drawn:

- sliding mode of variable e_V is successfully enforced;
- *reaching time* (defined in the Sliding Mode literature as the time needed by σ to reach zero for the first time) is linearly decreasing with observer gain: it is roughly 1.5s, 15s and 150s, respectively, for $m = 10^{-2}$, 10^{-3} and 10^{-4};
- on the other hand, the higher is m, the more evident are oscillations around zero of the sliding variable, especially towards the end of simulation (where output equation is more non-linear); in other words, lower values of m entail a longer *reaching time*, but a more stable estimation;
- as depicted in Figure 8, during sliding, injection variable v exhibits high-frequency switching, which is typically named *chattering phenomenon* in Sliding Mode literature; this phenomenon is usually not critical for estimation problems.

Thanks to the designed SMO algorithm, not only e_V is driven to zero, but also all state estimation errors defined earlier (and all other elements along r, not shown here for space reasons). The result of state estimation convergence are presented in Figure 9 for surface concentrations and in Figure 10 for core concentrations. Notice that the same properties described for e_V hold true in these cases as well. Given the convergence of state estimations, it follows immediately that SoC estimation is also converging, with the same properties as observed above, as shown in Figure 11.

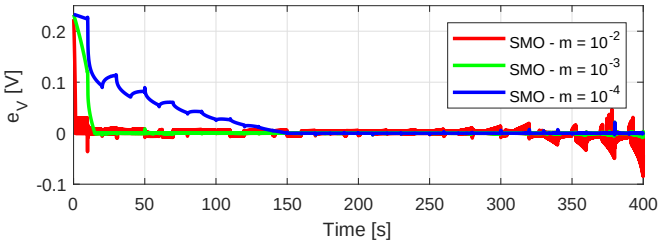

Fig. 7. Output voltage estimation error for SMO with mass-preserving correction, for different values of gain m.

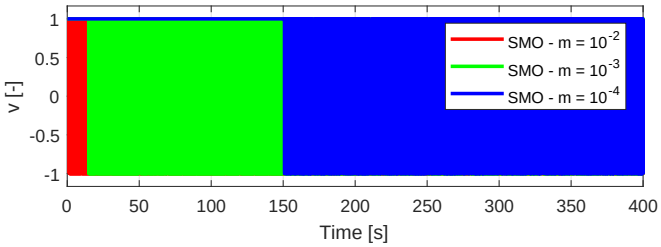

Fig. 8. Injection variable for SMO with mass-preserving correction, for different values of gain m.

To test the mass-preserving SMO estimation robustness, the above test is repeated with additive measurement noise acting on V. The noise is white, with null mean and variance equal to 1mV. Even in this scenario, state estimation errors converge to zero. However, the following considerations are due:

- reaching time is longer than without measurement noise;
- oscillations are present on state estimates, as expected, along the entire duration of the test, which are filtered by lower values of gain m;

As such, a trade-off is clearly observed, which was less prominent without noise: a lower gain m leads to slower convergence of state estimates, but also to less noisy signals (filtering effect of state observer is enhanced).

V. Conclusions

In the present work, a SMO is applied to the electrochemical SPM. A mass-preserving design algorithm is proposed for the choice of the SMO gain matrix. This enables to overcome the weak observability issues associated with SPM, and to successfully estimate lithium concentrations profiles along particles radii and bulk State of Charge. The obtained results are confirmed with noisy output voltage measurements.

As a future work, the algorithm robustness w.r.t. model parametric uncertainty may be investigated as well. Also, further oscillations suppression in estimated states may be achieved by designing a second-order SMO. A natural application of the proposed algorithm is the implementation on a real-world BMS, thanks to its inherent computational efficiency.

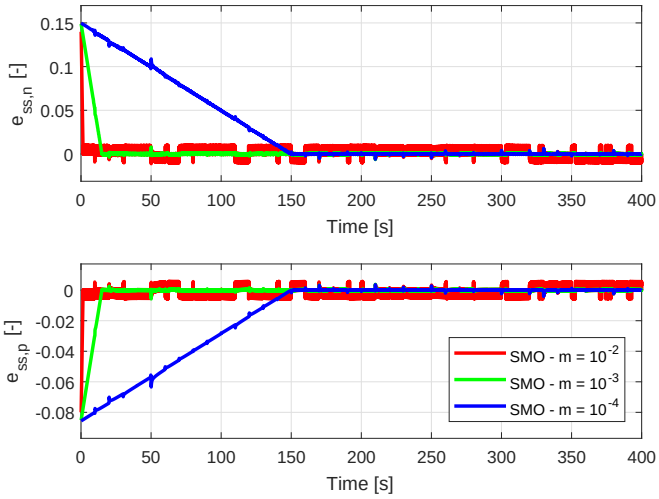

Fig. 9. Negative electrode state estimation errors for SMO with mass-preserving correction (top: negative electrode; bottom: positive electrode), for different values of gain m.

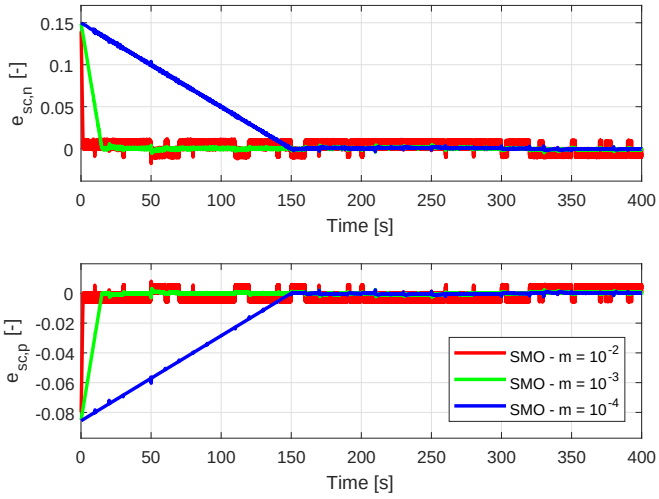

Fig. 10. Positive electrode state estimation errors for SMO with mass-preserving correction (top: negative electrode; bottom: positive electrode, for different values of gain m).

References

[1] Karthik Somasundaram, Erik Birgersson, and Arun Sadashiv Mujumdar. Thermal–electrochemical model for passive thermal management of a spiral-wound lithium-ion battery. *Journal of Power Sources*, 203:84–96, 2012.

[2] Nalin A Chaturvedi, Reinhardt Klein, Jake Christensen, Jasim Ahmed, and Aleksandar Kojic. Algorithms for advanced battery-management systems. *IEEE Control Systems*, 30(3):49–68, 2010.

[3] Paul WC Northrop, Bharatkumar Suthar, Venkatasailanathan Ramadesigan, Shriram Santhanagopalan, Richard D Braatz, and Venkat R Subramanian. Efficient simulation and reformulation of lithium-ion battery models for enabling electric transportation. *Journal of The Electrochemical Society*, 161(8):E3149–E3157, 2014.

[4] K. A. Smith, C. D. Rahn, and C. Y. Wang. Model-based electrochemical estimation and constraint management for pulse operation of lithium ion batteries. *IEEE Transactions on Control Systems Technology*, 18(3):654–663, May 2010.

[5] Marc Doyle, Thomas F Fuller, and John Newman. Modeling of galvanostatic charge and discharge of the lithium/polymer/insertion cell. *Journal of the Electrochemical Society*, 140(6):1526–1533, 1993.

[6] Kandler Smith and Chao-Yang Wang. Solid-state diffusion limitations on pulse operation of a lithium ion cell for hybrid electric vehicles. *Journal of Power Sources*, 161(1):628–639, 2006.

[7] Kandler A Smith, Christopher D Rahn, and Chao-Yang Wang. Control oriented 1d electrochemical model of lithium ion battery. *Energy*

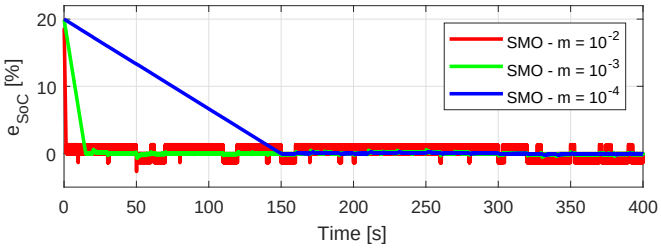

Fig. 11. State of Charge estimation errors for SMO with mass-preserving correction, for different values of gain m.

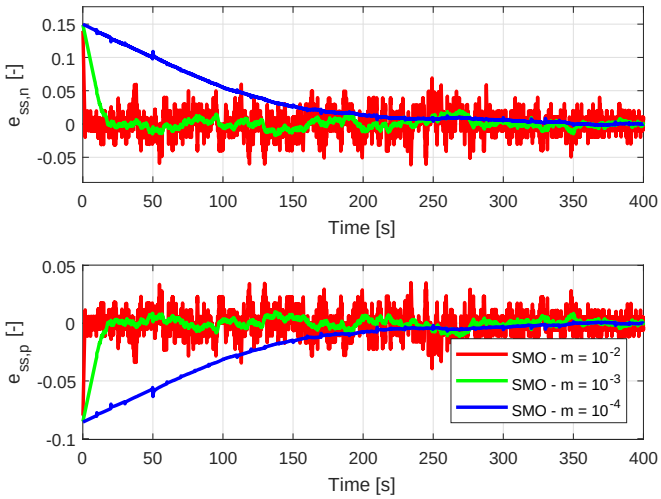

Fig. 12. Negative electrode state estimation errors for SMO with mass-preserving correction and noisy measurements (top: negative electrode; bottom: positive electrode), for different values of gain m.

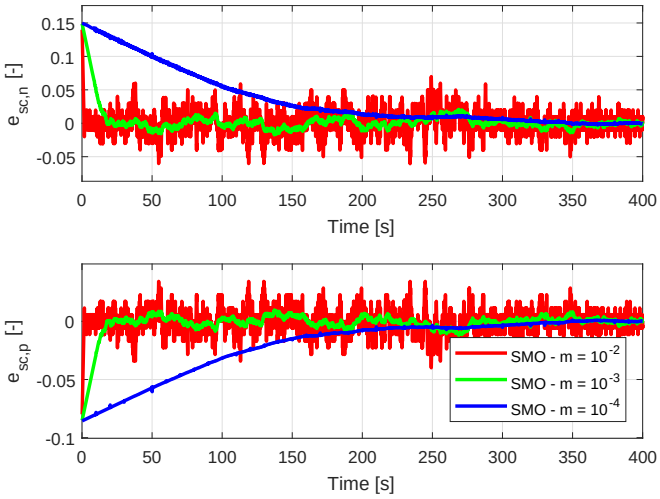

Fig. 13. Positive electrode state estimation errors for SMO with mass-preserving correction and noisy measurements (top: negative electrode; bottom: positive electrode, for different values of gain m).

Conversion and management, 48(9):2565–2578, 2007.

[8] Venkatasailanathan Ramadesigan, Vijayasekaran Boovaragavan, J Carl Pirkle, and Venkat R Subramanian. Efficient reformulation of solid-phase diffusion in physics-based lithium-ion battery models. *Journal of The Electrochemical Society*, 157(7):A854–A860, 2010.

[9] Shriram Santhanagopalan, Qingzhi Guo, Premanand Ramadass, and Ralph E White. Review of models for predicting the cycling performance of lithium ion batteries. *Journal of Power Sources*, 156(2):620–628, 2006.

[10] Venkat R Subramanian, Vinten D Diwakar, and Deepak Tapriyal. Efficient macro-micro scale coupled modeling of batteries. *Journal of The Electrochemical Society*, 152(10):A2002–A2008, 2005.

[11] Yuri Shtessel, Christopher Edwards, Leonid Fridman, and Arie Levant. *Sliding mode control and observation*, volume 10. Springer, 2014.

[12] Sarah K Spurgeon. Sliding mode observers: a survey. *International Journal of Systems Science*, 39(8):751–764, 2008.

[13] Xiaopeng Chen, Weixiang Shen, Zhenwei Cao, and Ajay Kapoor. A novel approach for state of charge estimation based on adaptive switching gain sliding mode observer in electric vehicles. *Journal of Power Sources*, 246:667–678, 2014.

[14] Scott J Moura, Nalin A Chaturvedi, and Miroslav Krstic. Pde estimation techniques for advanced battery management systems, part i: Soc estimation. In *American Control Conference (ACC), 2012*, pages 559–565. IEEE, 2012.

[15] Matteo Corno, Nimitt Bhatt, Sergio M Savaresi, and Michel Verhaegen. Electrochemical model-based state of charge estimation for li-ion cells. *IEEE Transactions on Control Systems Technology*, 23(1):117–127, 2015.

[16] Adrien M. Bizeray, Shi Zhao, Stephen Duncan, and David A. Howey. Lithium-ion battery thermal-electrochemical model-based state estimation using orthogonal collocation and a modified extended kalman filter. *CoRR*, abs/1506.08689, 2015.

[17] Gregory L Plett. Sigma-point kalman filtering for battery management systems of lipb-based hev battery packs: Part 1: Introduction and state estimation. *Journal of Power Sources*, 161(2):1356–1368, 2006.

[18] Shriram Santhanagopalan and Ralph E. White. State of charge estimation using an unscented filter for high power lithium ion cells. *International Journal of Energy Research*, 34(2):152–163, 2010.

[19] S. J. Julier, J. K. Uhlmann, and H. F. Durrant-Whyte. A new approach for filtering nonlinear systems. In *American Control Conference, Proceedings of the 1995*, volume 3, pages 1628–1632 vol.3, Jun 1995.

[20] Satadru Dey, Beshah Ayalew, and Pierluigi Pisu. Combined estimation of state-of-charge and state-of-health of li-ion battery cells using smo on electrochemical model. In *Variable Structure Systems (VSS), 2014 13th International Workshop on*, pages 1–6. IEEE, 2014.